JOURNAL OF CATALYSIS 143, 201–214 (1993)

Chromia Supported on Titania
I. An EPR Study of the Chemical and Structural Changes Occurring during Catalyst Genesis

K. KÖHLER,* C. W. SCHLÄPFER,* A. VON ZELEWSKY,* J. NICKL,† J. ENGWEILER,† AND A. BAIKER†

*Institute of Inorganic and Analytical Chemistry, University of Fribourg, Pérolles, CH-1700 Fribourg, Switzerland; and †Department of Chemical Engineering and Industrial Chemistry, Swiss Federal Institute of Technology, ETH-Zentrum, CH-8092 Zürich, Switzerland

Received October 26, 1992; revised February 9, 1993

The chemical and structural changes occurring during the preparation of chromia on titania catalysts have been investigated using electron paramagnetic resonance (EPR). The various chromium species after impregnation, calcination in excess oxygen, and temperature-programmed reduction were characterized. Catalysts with chromia contents ranging from 0.1 to 32 wt% were prepared by impregnation of titania with aqueous solutions of $Cr(NO_3)_3 \cdot 9H_2O$. After impregnation, mononulear, dinuclear (δ-signal), and polynuclear (β-signal) Cr(III) surface complexes as well as Cr(V) species (γ-signal) were observed. The EPR spectra of the calcined catalyst consist of a broad line at $g = 1.98$ (β-signal) assigned to magnetically interacting Cr(III) surface ions and the narrow γ-signal with $g_\perp = 1.975$ and $g_\parallel = 1.955$–1.964 corresponding to Cr(V) surface complexes. The intensities and linewidths of the signals are strongly dependent on chromium content, preparation conditions, recording temperature (77–423 K), and the microwave frequency ($\nu = 9.5$ and 35 GHz), and are interpreted in terms of dipolar and exchange interactions and exchange narrowing due to different Cr_2O_3 cluster sizes. The Cr(V) complexes are antiferromagnetically exchanged coupled to other surface species as deduced from the temperature dependence of the γ-signal. For higher Cr contents (>5 wt% Cr_2O_3/TiO_2), the simultaneous existence of antiferromagnetic α-Cr_2O_3 and ferromagnetic CrO_2 crystallites on the surface is proposed. At temperatures >773 K, Cr(III) ions are partially incorporated into the rutile and anatase lattice. A considerable amount of chromium is oxidized to Cr(VI) by calcination. The relative intensities of the EPR signals were determined.

1. INTRODUCTION

Electron paramagnetic resonance (EPR) spectroscopy is a valuable tool for the characterization of catalysts containing transition metal ions. Especially chromia supported on metal oxides has been the subject of many spectroscopic investigations. Concerning EPR, it is a fortunate circumstance of nature that most chromia catalysts consist (mainly) of paramagnetic chromium species diamagnetically diluted by the carrier.

In the present work, we report the results of EPR investigations of CrO_x/TiO_2 catalysts which are of interest for the selective catalytic reduction of nitric oxide by ammonia in excess oxygen (*1*). There are several reports on EPR investigations of chromium species on the surface of TiO_2 and incorporated into the lattice of the modifications rutile (*2, 3*), anatase (*4, 5*) and brookite (*6*) in the literature. To our knowledge, however, there is no systematic EPR work on CrO_x/TiO_2 catalysts up to now which includes the dependence of EPR spectra on total chromium content, preparation conditions, recording temperature, and microwave frequency. This paper describes the effects of impregnation (with $Cr(NO_3)_3 \cdot 9H_2O$), oxidative calcination, and temperature-programmed reduction on the EPR spectra taken at X-band and Q-band frequencies and

0021-9517/93 $5.00

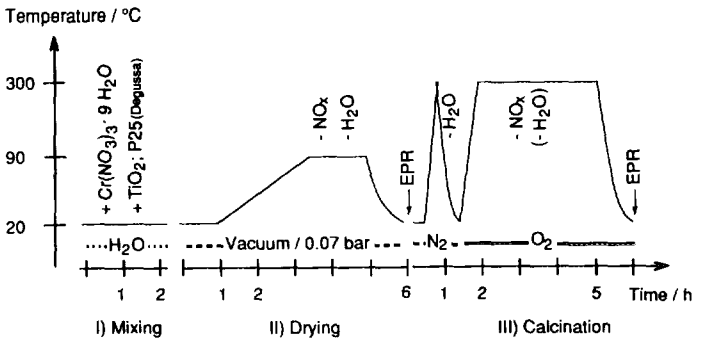

FIG. 1. Schematic presentation of catalyst genesis.

at temperatures between 77 and 423 K. The investigations of the impregnated carrier before calcination, which is in general not reported in similar papers, have made valuable contributions to the understanding of the whole system, and is therefore also considered in detail.

Most of the typical generally overlaid spectral patterns described are well known from the literature, but were obtained under more or less different preparation conditions and were not always interpreted in the same manner. Starting from extensive investigations of the CrO_x/Al_2O_3 system in the 1950s and 1960s (*7*), these spectral patterns have been designated by Greek letters. This nomenclature has been widely accepted, especially in the catalysis literature for similar systems, e. g., CrO_x/SiO_2 (*8*), CrO_x/ZnO (*9, 10*), or CrO_x/ZrO_2 (*11*). For compatibility and easier understanding, we use as far as possible the same designation in this paper.

2. EXPERIMENTAL

Catalyst preparation. A schematic presentation of the catalyst genesis is shown in Fig. 1. TiO_2 P25 (specific surface area: 49 m^2/g, anatase/rutile ratio 7 : 3, supplier Degussa, Germany) was used as a carrier. The impregnation of the carrier was performed by addition of different amounts of $Cr(NO_3)_3 \cdot 9H_2O$ (Fluka, Switzerland) dissolved in distilled water to an aqueous TiO_2 slurry under vigorous stirring for 2 h. Subsequently water was removed at 50 Torr (6.66 $\times 10^3$ Pa) by slowly heating to 363 K within 4 h. After breaking and sieving to 0.3 to 0.5 mm grain size, catalysts were rapidly heated in a nitrogen stream (50 ml/min) to 573 K, cooled down to room temperature, and then calcined in an oxygen stream (50 ml/min) at 573 K for 3 h. Catalysts with chromia contents of 0.1, 0.5, 1, 2, 3, 5, 10, 16.6, and 32 wt% (referred to wt% Cr_2O_3 per total catalyst weight) have been prepared (Table 1). EPR investigations were performed with samples in the status indicated in Fig. 1.

Temperature-programmed reduction (TPR) was carried out using hydrogen as reductant (6% H_2 in Ar stream), whereby

TABLE 1

Composition[a] of the Supported CrO_x Samples[b]

Sample	wt% Cr_2O_3/TiO_2	n_{Cr} [mol/g] TiO_2[c]
1	0.1	1.3×10^{-5}
2	0.5	6.6×10^{-5}
3	1.0	1.3×10^{-5}
4	2.0	2.7×10^{-4}
5	3.0	4.1×10^{-4}
6	5.0	6.9×10^{-4}
7	10.0	1.5×10^{-3}
8	16.6	2.6×10^{-3}
9	32.0	6.2×10^{-3}

[a] Starting composition for impregnation.
[b] In this paper, all data concerning total chromium content (wt%) used in the text are referred to wt% Cr_2O_3 per total catalyst weight, as column 2.
[c] Rounded values.

the temperature was ramped from 298 to 973 K at 10 K/min.

The BET surface area of all calcined samples was found to be within 45–50 m^2/g.

EPR measurements. EPR spectra were recorded on a Bruker ESP300 system at X-band frequency (Varian E-9 spectrometer at Q-band frequency) at temperatures between 77 (130) and 420 (373) K in quartz tubes under atmospheric pressure or in vacuum (10^{-1} Torr, see later). In general, the spectra were measured at a microwave frequency of about 9.4 (35.0) GHz, with microwave powers of 1–5 mW (Q-band, attenuation: 8 dB), with a modulation amplitude of 0.2 (0.4) mT, and a modulation frequency of 100 (100) kHz. The data in parentheses refer to the Q-band measurements. The g values were determined with a NMR magnetometer and DPPH as a g marker. The measurements were carried out in a Bruker TE102 standard rectangular cavity, in a Bruker TE104 double rectangular cavity (both X-band), and in a modified Varian E-266 Q-band TE011 (right circular cylinder) cavity, respectively.

The relative spin concentrations of the various chromium species were determined using the double rectangular cavity and DPPH as the reference sample. The catalyst samples of constant weight were measured in quartz tubes of defined diameter. The intensity of the different signals was obtained by numerical double integration using the ESP300 software (base line correction, background fit, and spectra subtraction).

3. RESULTS

3.1. Impregnated TiO_2

The β-signal. The room temperature EPR spectra of the catalyst after impregnation (Fig. 2) for all Cr contents >0.1 wt% consist of a broad symmetric line of differing line widths close to Lorentzian in shape and centered at $g = 1.98$ (superimposed by the γ- and δ-signal, see below). The dependence of the peak-to-peak linewidth ΔB_{pp} of this broad line on the chromium content is shown in Fig. 3. For Cr contents up to 2 wt%, the linewidth at X-band is constant (45 mT); it increases for higher concentrations up to 62 mT, but is remarkably reduced for Cr contents of 10 wt% and higher (down to 21 mT for 32 wt%, value not shown). At Q-band frequencies, ΔB_{pp} is clearly reduced in comparison to X-band for lower concentrations of chromium, nearly unchanged for higher contents, and the reverse relation is found for 32 wt% (ΔB_{pp}: X, 21 mT; Q, 38 mT). The linewidth of the signal increases by about 10 % for all Cr contents when going

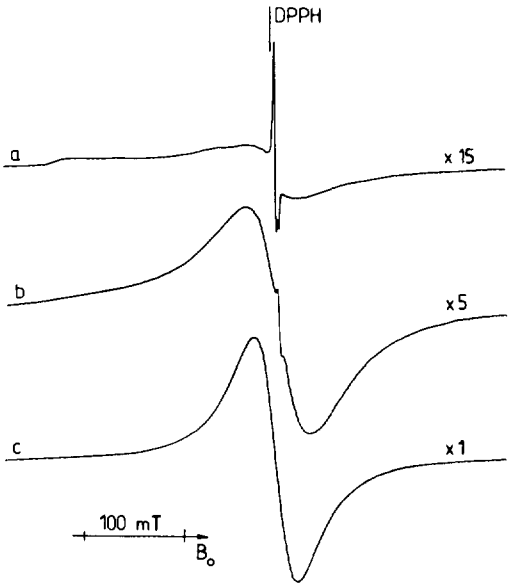

FIG. 2. EPR spectra of the impregnated TiO_2 at T = 293 K, (a) 1 wt%, (b) 5 wt%, and (c) 16.6 wt%.

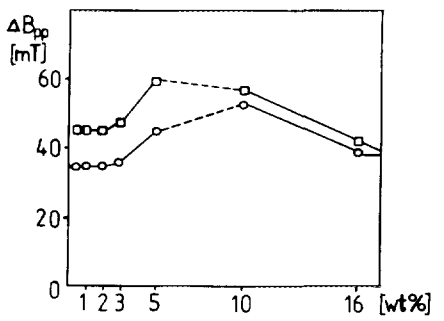

FIG. 3. Linewidths of the β-signal of the impregnated samples at X-band (□) and Q-band (○) for different total chromium contents (wt%); T = 293 K.

from room temperature to T = 120 K, and the integrated intensity increases by a factor of 1.5 to 2.

By treatment of the impregnated TiO_2 with boiling aqueous Na_2EDTA solution, the signal is partially or nearly completely removed depending on duration of the treatment and on Cr content. This procedure yields pink supernatant solutions of the well known Cr(III) EDTA complex. The samples with Cr contents <3 wt% (ΔB_{pp} = 45 mT) show an increased linewidth at X-band (ΔB_{pp} = 53 mT) after suspending in water, centrifuging, and air drying. A similar, but less pronounced effect could be observed after storing the samples over several months in closed vessels.

In the literature, the broad symmetric line is generally designated as the $\beta^{(')}$-signal and assigned to clustered Cr_2O_3 of different cluster sizes on oxidic surfaces (*7, 9, 11–13*). There is, however, a difference between the range of line width change of the β-signal reported for other (but calcined) systems (e.g., Al_2O_3, 200–80 mT (*7, 12*); ZrO_2, 180–150 mT (*11*) and that observed by us. On the other hand, our linewidths especially for smaller Cr contents are very similar to those reported for chromium(III) species adsorbed or ion-exchanged on SiO_2 (*13*), Al_2O_3 (*14*), or on several mineral clays (*15*). The signals were assigned to polymeric chromia (i.e., some condensation product of $[Cr(H_2O)_6]^{3+}$) on SiO_2 (*13*) or to isolated surface complexes of Cr(III) with more or less disturbed octahedral symmetry on the other surfaces (*14, 15*). In the latter case it is argued that the EPR signals of the Cr(III) surface species are not significantly temperature dependent, whereas it is known that the linewidth of Cr(III) polymers changes dramatically upon cooling down to liquid-helium temperature (*15*). Because we have no measurements in this temperature range, we cannot decide whether the β-signal observed for low Cr contents (i.e., <2 wt%, ΔB_{pp} = 45 mT) should be assigned to small condensation products of Cr(III) or to single Cr(III) ions with more or less disturbed octahedral symmetry. Isolated Cr(III) ions in relatively strong axial crystal fields with or without distortions of lower symmetry should give rise to an EPR spectrum rather comparable to that of the δ-signal (see below) (*12–14, 16*). However, based on the spectroscopic features and preparation conditions, we tend to assign the β-signal for Cr contents >2 wt% rather to polynuclear Cr(III) species on the surface of TiO_2.

In summary, we interpret the linewidths effects as follows. At lower Cr contents, isolated, not magnetically interacting Cr(III) complexes (and/or small polynuclear condensation products), are responsible for the β-signal (constant line widths). Dipolar interactions between the Cr(III) ions of one cluster of increasing size (and between different clusters) broaden the line up to a point where spin exchange coupling causes exchange narrowing of the resonance, partially "washing out" the diplar line broadening. The observed linewidth dependence is in agreement with corresponding quantitative expressions for the simultaneous action of dipolar and exchange fields, which are given in the literature (*17, 18*).

A linewidth variation with the frequency (in our case: ν = 9.5 and 35 GHz) of magnetically interacting systems similar to the one observed by us is discussed in the literature in terms of the relation between observation frequency (or field B_0) and exchange frequency (or field B_e) (compare Van Vleck (*17*) and Anderson and Weiss (*18*)). Similar results were reported by Scaringe and Kokoszka (*19*) for the mixed valence system Cr(III)–Cu(I–II) and interpreted in the same manner. In fact, the linewidth of the β-signal in Q-band is larger than in X-band in all cases, where we assume that the exchange forces dominate over the dipolar interactions (*20*).

The δ-signal. For lower chromium contents (>5 wt%), additional broad absorptions of low intensity distributed over a wide field range between 100 and 300 mT (ν = 9.5 GHz) with maxima at about 150 (and 270) mT were observed (Fig. 2a). The corre-

sponding species can be washed out by Na_2EDTA/H_2O treatment. At Q-band frequencies, this spectral pattern is not observable. The integrated intensity increases with decreasing temperature as expected from the Curie law to a first approximation. The linewidth of the δ-signal remains constant for all temperatures. The relative intensity of the δ-signal to the β-signal reaches about 20% for 1 wt% Cr content and is less than 10% of the β-signal for 2 to 5 wt%.

These low field absorptions are designated as the δ-signal in the literature and assigned to isolated Cr(III) ions (or dimers) in relatively strong axial crystal fields with distortions of lower symmetry for the systems CrO_x/Al_2O_3 (*12*) and CrO_x/SiO_2 (*13*). On ZrO_2, however, isolated Cr(III) ions on the surface (after calcination) were excluded because of the conditions of their formation, and a similar pattern was assigned to exchange coupled Cr(III) ions and the spectra were explained by the combined effect of zero-field, dipolar and exchange interactions. The fact that there is no δ-signal observable at frequencies higher than 9.5 GHz (i.e., at K- or Q-band) was explained by O'Reilly and Maclver (*12*) in terms of the remarkable diminuation of the resonance due to the greater range of field strength spanned by the resonance. According to this argument and taking into account the formation conditions, we assign the δ-signal observed by us to single or dimeric Cr(III) complexes with a variety of different coordination spheres (strong axial crystal fields and/or other distortions).

The γ-signal. For chromium contents up to 5 wt%, the β-resonance is superimposed by a narrow line of $g_{(\perp)} = 1.975$ (±0.002) with a line width varying within 2–3.5 mT. This line is asymmetric or the anisotropy is resolved ($g_\perp = 1.975$, $g_\parallel = 1.964$–1.955 ± 0.002) depending on linewidth and chromium content (larger linewidths for higher Cr contents). The same parameters are also derived from the analysis of the Q-band spectra where the asymmetry (or "anisotropy") is more pronounced, as expected.

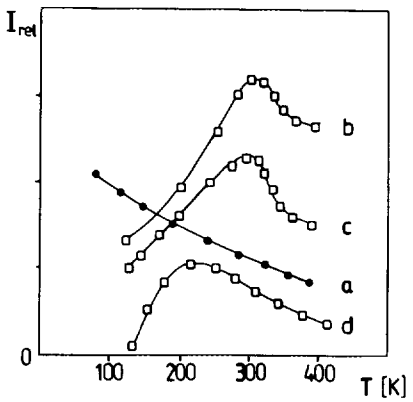

FIG. 4. Temperature dependence of the γ-signal (Cr(V)) of the impregnated (○) and calcined catalyst (□) for chosen total chromium contents: (a) 1 wt%, (b) 1 wt%, (c) 2 wt%, and (d) 5 wt%. The relative intensities at room temperature are slightly shifted toward each other for better clarity.

After treating the impregnated catalyst with organic solvents (suspensions in acetic acid, acetonitrile, or methylene chloride) under different conditions (room temperature or boiling suspensions, 30 min), the anisotropy is always resolved and one obtains $g_\perp = 1.975$, $g_\parallel = 1.959$. Treatment with water (suspensions) removes the signal partially or completely depending on the time and the temperature of the treatment. The γ-signal undergoes reversible broadening in the presence or absence (vacuum) of oxygen at room temperature, respectively. The temperature dependence of the signal shows a different behaviour for different Cr contents: for lower ones, it is not changed in shape at $T = 110$ K compared to room temperature, and its intensity increases as approximately expected from the Curie law for paramagnetic species (Fig. 4a). For 2 to 5 wt% the signal intensity decreases when the temperature is lowered, in the latter case remarkably such that at $T = 77$ K the signal cannot be observed. This temperature effect is qualitatively independent of the oxygen content of the gaseous phase. Taking this into account, the relative intensities at room temperature shown in Fig. 5 must be used carefully and are probably not suitable for

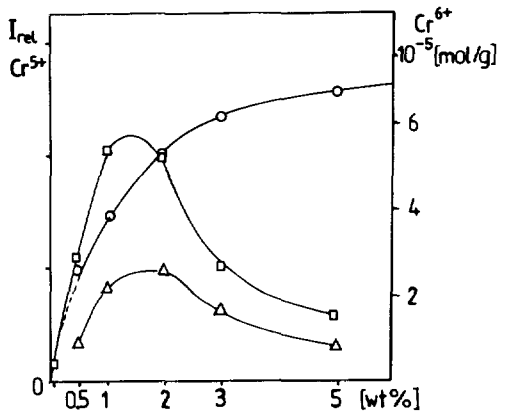

FIG. 5. Relative intensity of the γ-signal (Cr(V)) of the impregnated (Δ) and calcined ($\square$) samples and Cr(VI) content ($\bigcirc$, 10^{-5} mol/g calcined catalyst) for different total chromium contents (wt%).

the determination of the actual Cr(V) concentrations, at least not for higher total chromium contents.

In most cases, the narrow asymmetric line (or powder spectrum) with $g_{(\perp)} = 1.975$, the so-called γ-signal, is assigned to single Cr(V) species ($3d^1$, $S = \frac{1}{2}$) of different coordination sphere (square pyramidal or distorted tetrahedral) on the surface of the corresponding oxide (*8, 11–13, 21*). Because of the different relaxation times expected for square pyramidal and tetrahedral coordination, the γ-signal observed at room temperature is generally assigned to Cr(V) in square pyramidal coordination. A detailed spectroscopic investigation was reported for the system CrO_x/SiO_2 by van Reijen and Cossee (*8*). However, the γ-signal is also attributed to trimers of mixed valency "Cr(VI)–O–Cr(III)–O–Cr(VI)" (average oxidation number +5) by Spitz (*12*) as well as by Ellison and Sing (*23*) for CrO_x/Al_2O_3, and a similar model has been proposed by Evans and co-workers for CrO_x/TiO_2 (rutile) (*3, 4*). However, also by other authors the idea was expressed that the γ-signal is at least partially associated with the β-phase chromium (*7*). Cimino *et al.* (*11*) concluded from the disagreement of the fraction of Cr(V) observed by EPR and the average oxidation number determined by chemical methods that especially for more concentrated systems, a fraction of Cr(V) complexes on the surface of ZrO_2 escapes EPR detection because of magnetic interactions with other Cr(V) species. In fact, Cordischi *et al.* (*24*) could observe exchange coupled isolated pairs of Cr(V) on ZrO_2 by EPR at 77 K and at room temperature.

From the temperature dependence of our γ-signal, we deduce that for the lowest Cr contents isolated surface Cr(V) species with probably square pyramidal coordination are responsible for the signal. At higher Cr contents, however, these Cr(V) complexes are antiferromagnetically exchange coupled to Cr(III) (β-phase) or to Cr(V) species.

The ratio between detected Cr(V) ($S = \frac{1}{2}$) and Cr(III) ($S = \frac{3}{2}$) species calculated from the integrated intensities reaches from at most 20% Cr(V) for lower to 3% for higher Cr contents. No γ-signal was observed for Cr contents >5 wt%.

Cr(VI). Only traces of Cr(VI) could be found by the method proposed in Ref. (*3*): treatment with 1,2-dihydroxyethane gives a very weak EPR signal of the corresponding bis-ethane-1,2-diolatochromate(V) complex in the suspension as well as in the supernatant solution after centrifugation.

3.2. Calcined Catalyst

Typical EPR spectra of the catalyst after calcination at 573 K in an oxygen stream for chosen chromium contents are shown in Fig. 6. Similar to those of the impregnated TiO_2, they consist of an overlay of two or more spectra. The spectral patterns strongly depend on total chromium content and recording temperature, and are described and discussed separately. We assign the spectra to different kinds of Cr(III), Cr(IV), and Cr(V) species on the surface of TiO_2.

Cr(III) species. (a) *Cr contents up to 0.5 wt%*: No Cr(III) signals were observed, i.e., the spectra consist of the narrow γ-signal only (see below). However, as indicated by double integration, some amount of Cr(III) seems to be latent because of the broadness expected for the Cr(III) resonance.

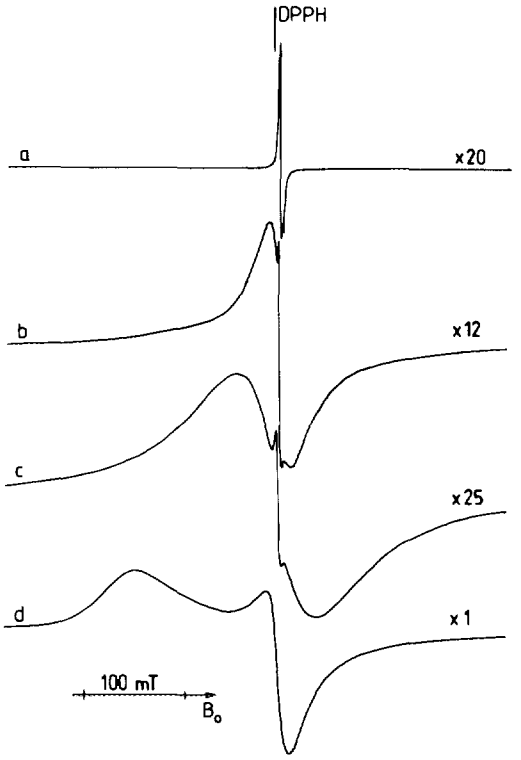

FIG. 6. EPR spectra after calcination in O_2 at T = 573 K. Recording temperature, 293 K: (a) 0.5 wt%, (b) 2 wt%, (c) 5 wt%, (d) 10 wt%.

(b) *Cr contents from 1 to 5 wt%*: The linewidths at room temperature for X- and Q-band are given in Fig. 7. For 1 and 2 wt%, the lines are smaller compared to the β-signal of the impregnated catalysts, whereas

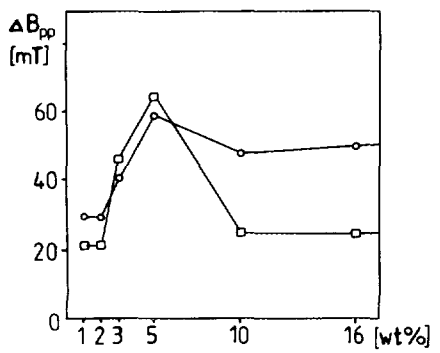

FIG. 7. Linewidth of the signals at about g = 1.98–1.97 of the calcined samples at X-band (□) and Q-band (○) frequencies for different total chromium contents (wt%).

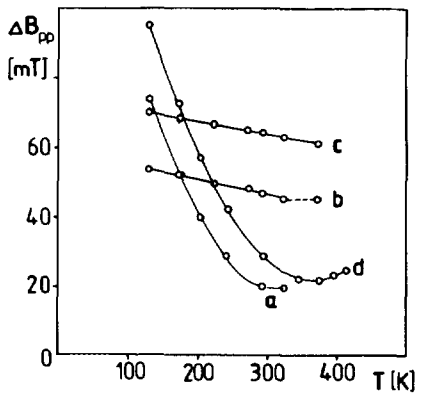

FIG. 8. Temperature dependence of the line widths of the broad signals at g = 1.98–1.97 for chosen total chromium contents after calcination: (a) 2 wt%, (b) 3 wt%, (c) 5 wt%, and (d) 10 wt%.

the lines for 3 and 5 wt% are clearly broadened. The most remarkable feature of all calcined samples is the temperature dependence of the linewidths and integrated intensities of the broad β-lines centered at about g = 1.98 (Figs. 8 and 9). The corresponding temperature dependence for 3 and 5 wt% is similar to that of the β-signal of the impregnated TiO_2.

According to its spectroscopic features (g value, linewidth, variation of intensity with recording temperature), this β-signal observed for Cr contents between 3 and 5 wt% is assigned to clustered, but amorphous Cr_2O_3. The increased linewidth in comparison to the impregnated samples (3–5 wt%) is interpreted in terms of an increase of the cluster sizes by calcination. It cannot be explained by dipolar interactions of isolated Cr(III) species, because the number of Cr(III) complexes decreases upon calcination. The spectroscopic features are similar to that found for the pure precursor decomposed at 498 K in air. The size of the Cr_2O_3 clusters is too small to allow for collective properties of the samples, i.e., there is not yet long-range antiferromagnetic order as for higher Cr contents and α-Cr_2O_3, respectively.

For the 1 and 2 wt% samples, the temperature dependence of the EPR spectra is very striking, as shown in Figs. 8 and 9. The intensity increases with decreasing temper-

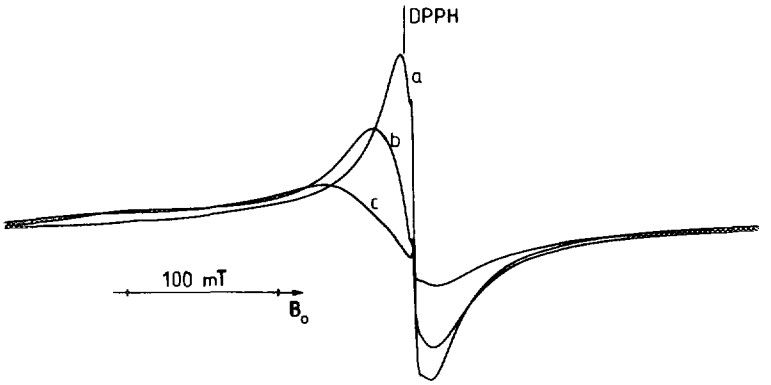

FIG. 9. EPR spectrum for the calcined 2 wt% sample for different recording temperatures: (a) 293 K, (b) 203 K, and (c) 130 K.

ature down to a temperature where it reaches a maximum ($T \approx 200$ K), and then it decreases with further decreasing temperature. The line broadening with decreasing temperature is an asymmetric one (Fig. 9). The behaviour of the signal intensity and linewidth for these Cr contents is similar to that found for high-surface-area Cr_2O_3 (*25*). Upon lowering the recording temperature, the EPR signal became progressively broader, disappearing at about 280 K (for comparison: T_N of α-Cr_2O_3: 308 K). An average particle size of 7 nm was calculated from these results. The T_N values found for the system under study are still lower and less pronounced. We attribute this to clusters of smaller sizes.

(c) *Cr contents >5 wt%*: The X-band EPR spectra for 10, 16.6, and 32 wt% consist of a 20–30 mT broad line at $g = 1.97$, and a strong absorption at about 200 mT (Fig. 6d). The spectral pattern is strongly temperature dependent in respect to the linewidth of the derivative line and the integral intensity of the complete spectrum, as well as the field position of the absorption line. Starting at $T = 350$ K, a single 20-mT broad resonance (derivative line) is broadened asymmetrically with decreasing temperature (Fig. 8d), and the absorption peak mentioned above "moves" out of the derivative peak to lower fields. With further temperature decrease, the distance between these two lines increases up to a constant value of about 140 mT (Fig. 6d). The pure precursor calcined in the same manner shows a similar complex magnetic behaviour.

To our knowledge, behaviour of EPR spectra as described above has not been reported in the literature for supported Cr catalysts until now. It can only be explained taking into account collective properties of corresponding chromium oxide species (crystallites), but not only by the existence of antiferromagnetic α-Cr_2O_3. Simultaneous interaction with a ferromagnetic system such as CrO_2 could be a reason for the striking spectroscopic features (*26*). The proof of crystalline CrO_2 (besides Cr_2O_3) by X-ray diffraction of the calcined precursor is an additional indication. At this point of the investigation, we deduce the following. For concentrations of 10–32 wt%, the spectra and their temperature dependence must be explained by collective interactions of chromium oxide species (small crystallites, probably mainly antiferromagnetic α-Cr_2O_3). Also for Cr contents <10 wt%, the presence of some amount of Cr(IV) cannot be excluded. The Cr(IV) signal could be masked by that of Cr(III). Cr(IV) surface species ($3d^2$, $S = 1$) could give a similar spectral pattern to Cr(III), strongly dependent on its coordination sphere.

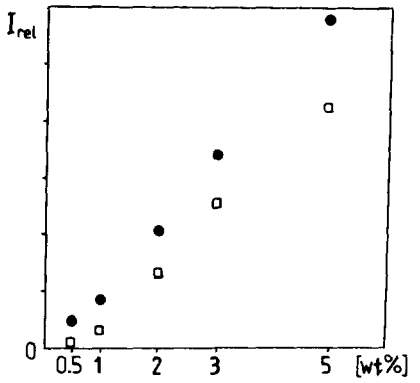

FIG. 10. Relative integral intensity of the Cr(III) EPR spectra at room temperature after impregnation (○) and calcination (□) for different chromium contents (wt%).

δ-Signal. The intensity of the δ-signal (compare Section 3.1.) is found to be zero or remarkably reduced in intensity after calcination, in contrast to the CrO_x/Al_2O_3 system (*12*). Probably, the corresponding single or dimeric Cr(III) surface complexes were involved in the formation of clustered Cr_2O_3, or they were oxidized to Cr(V) or Cr(VI) by calcination (O_2, 573 K).

The relative intensities of the Cr(III) species at room temperature before and after calcination are shown in Fig. 10. The Cr(III) concentration decreases upon calcination. The difference is in good qualitative agreement with the simultaneous increase of Cr(V) and Cr(VI) content (see below).

Cr(V) species: As already mentioned, the two samples with the lowest Cr content (0.1 and 0.5 wt%) show the γ-signal only. For higher Cr contents up to 5 wt%, the broad signals assigned to Cr(III) are superimposed by a γ-signal of different intensity. The linewidth (including the effect of reversible broadening in the presence/absence of O_2 at different temperatures), anisotropy, and g values of the γ-signal are very similar to those observed for the impregnated TiO_2 before calcination. The Cr(V) surface complexes are more stable with respect to disproportionation in water for calcined samples. The coordination sphere of the Cr(V) complexes changes by treatment with water as indicated by an overlay of γ-signals with about the same $g_\perp = 1.975$ but at least three different $g_\parallel$ values (1.955, 1.959, and 1.964). Table 2 contains selected EPR parameters of Cr(V) surface species obtained by us and gives a comparison with those found by other authors. By analogy with Section 3.1., we assign the γ-signal to Cr(V) surface complexes of different (square pyramidal) coordination. Figure 5 demonstrates that the intensity of the γ-signal is increased by calcination for all Cr contents shown. There is a maximum at about 1 or 2 wt%. However, the temperature dependence of the signal intensities shown in Fig. 4, which is qualitatively the same for all Cr contents 0.1–5 wt%, underlines the necessity to distinguish between the intensity of the γ-signal on the one hand and the actual number of Cr(V) species on the other hand. However, it can clearly be shown that the number of Cr(V) species is increased by calcination at least by a factor of about 2 (the stronger temperature dependence is found for the calcined samples). Exchange interactions between CrO_4^{3-} tetrahedra in the unit cell of Cr(V)-doped spodiosites becoming very significant with increasing Cr(V) concentration and decreasing temperature were described by Reinen *et al.* (*27*). For our system, we propose that the decrease in intensity of the

TABLE 2

EPR Parameters for Cr(V) Surface Complexes (γ-signal)

Carrier	Assignment	$g_\parallel$	$g_\perp$	Reference
TiO_2 (P25)	s.p.c.[a]	1.955 1.959 1.964	1.975	This paper
TiO_2		1.97		(*3*)
ZrO_2	s.p.c.	1.960	1.979	(*11*)
Al_2O_3	s.p.c.	1.955	1.975	(*21*)
SiO_2	s.p.c.	1.952	1.972	(*8*)
	th.c.[b]	1.898	1.975	(*8*)

[a] Cr(V) in square pyramidal coordination.
[b] Cr(V) in tetrahedral coordination.

γ-signal with decreasing temperature is due to an antiferromagnetic exchange coupling between Cr(V) and Cr(III) species (or clusters) or due to Cr(V)–Cr(V) interactions as observed by Cordischi *et al.* on ZrO_2 (*24*).

Cr(VI) species. By calcination, the colour of the samples changed from green (impregnated TiO_2) to yellow for lower or brown for higher Cr contents. A strong EPR signal of bis(ethane-1,2-diolato)chromate(V) was observed by stirring the calcined samples in 1,2-dihydroxyethane (*3*). In order to estimate the Cr(VI) content, we made the following simple experiment. Weighed samples were stirred in water (constant volume) until the extinction of the UV–vis spectrum remained constant (<30 min.). The spectrum obtained was identical with the one of CrO_3 in aqueous solution. The concentration of the supernatant solution after centrifugation was determined by calibration with CrO_3 in H_2O. The results are given together with the relative Cr(V) concentrations (EPR) in Fig. 5. Of course, this procedure contains some sources of error, e.g., the simultaneous disproportionation of Cr(V). However, it shows qualitatively that the Cr(VI) species form really the outermost surface layer, and they are only slightly connected to the surface or other surface species, respectively. In addition, the results are in good agreement with diffuse-reflectance-UV–vis investigations of the catalysts, which will be reported elsewhere.

In summary, the calcination of the impregnated TiO_2 oxidizes some Cr(III) to Cr(V) and Cr(VI) (and possibly to Cr(IV)). The absolute amount of Cr(VI) increases with increasing total chromium content, whereas the percentage (mol%) decreases in the same direction (Fig. 5 and Table 3). The ratio of detected Cr(V) to Cr(III) obtained by numerical double integration of the EPR signals is given in Table 3.

3.3. Temperature-Programmed Reduction (TPR)

Reduction profiles of the various calcined catalysts will be shown in Part II of this series (Ref. (*1*)). The calcined samples for Cr contents of 0.5, 2, and 10 wt% were measured after TPR up to a temperature of 973 K. The spectra for the lowest and the highest concentration at room temperature are shown in Fig. 11. In addition to Cr(V) species (0.5 wt%) and Cr(V) and Cr(III) surface species (broad line for 2 and 10 wt%), the spectral pattern of two other species, well-known from literature, are observed: (1) Cr(III) ions in rutile occupying cation sites vacated by Ti(IV) ions (*2*), and (2) Cr(III) at substitutional cation sites within anatase (*4*). The EPR parameters agree well with those reported by Amorelli *et al.* (*4*) for anatase and Evans *et al.* for rutile (*2*) and corresponding single-crystal data of Gerritsen *et al.* (*28*) and are not further discussed here.

For the lowest Cr content, nearly all chromium seems to be incorporated into the lattice(s) of TiO_2. However, a broad background observable at high receiver gain indicates some Cr(III) residue at the surface. The γ-signal overlaying the Cr(III) anatase spectrum is not detected at temperatures lower than 173 K, i.e., the pure Cr(III) anatase spectrum is then obtained. The same is true after treatment of the samples with water or Na_2EDTA solution, i.e., such a treatment removes the γ-signal (disproportionation, Fig. 12). The spectra of Cr(III) in anatase/rutile are not effected by treatment in boiling aqueous Na_2EDTA solution over 6 h. The broad symmetric line at $g = 1.98$ (β-signal) observed for 2 and 10 wt% is assigned to Cr(III) clusters of comparatively large size (ΔB_{pp} of this β-signal is larger than for all other Cr contents after calcination). This means that the TPR treatment (or the temperature of 973 K) effects a better distribution of the Cr(III) species on the surface for higher Cr contents since the striking spectral features observed for the corresponding calcined samples (before TPR), which were interpreted as arising from collective properties of crystallites of CrO_x, disappeared.

The ratio between Cr(III) in rutile and anatase is about 100 : 2 for 0.5 wt% and 100 : 8 for 10 wt%, respectively. This agrees

TABLE 3

Estimation of the Cr(VI) Content[a] and the Ratio of Cr(V) to Cr(III) Species Detected by EPR at Room Temperature[b] of the Calcined Catalyst

Sample	Cr content (wt%)	Cr(VI) (mol%)	Intensity ratio Cr(V):Cr(III)[b]
2	0.5	40	70:30
3	1.0	30	50:50
4	2.0	20	20:80
5	3.0	15	10:90
6	5.0	10	<5:95
7	10.0	7	No Cr(V) detected

Note. The relative error of both determinations is comparatively large (±10%); consequently, only rounded values are given.

[a] After resolution in water (see text).

[b] By comparison of the integrated intensities according to $N_A/N_B = [g_B^2 \cdot S_B (S_B + 1) \cdot \text{area(A)}]/[g_A^2 \cdot S_A(S_A + 1) \cdot \text{area(B)}]$.

well with the statement of Amorelli *et al.* (*4*) that the migration of Cr^{3+} ions (having a similar ionic size as Ti^{4+}) from the surface into the crystal lattice at temperatures > 773 K is clearly more difficult for anatase than for rutile because of structural differences (open channels in the rutile structure). This is underlined by our results, especially taking into account that TiO_2 P25 consists of about 30% rutile only, but 70% anatase.

No Cr(VI) is found after TPR treatment, that is, whereas Cr(VI) is reduced completely by H_2 at least a small residue of Cr(V) species (antiferromagnetically exchange coupled to other surface species) is always present after reduction with H_2.

4. DISCUSSION

Scheme 1 summarizes the various chromium species (directly or indirectly) observed by EPR after the different stages of preparation and treatment of the CrO_x/TiO_2 system.

By the impregnation procedure, the precursor $Cr(NO_3)_3 \cdot 9H_2O$ is partially decomposed and some Cr(III) is oxidized to Cr(V)

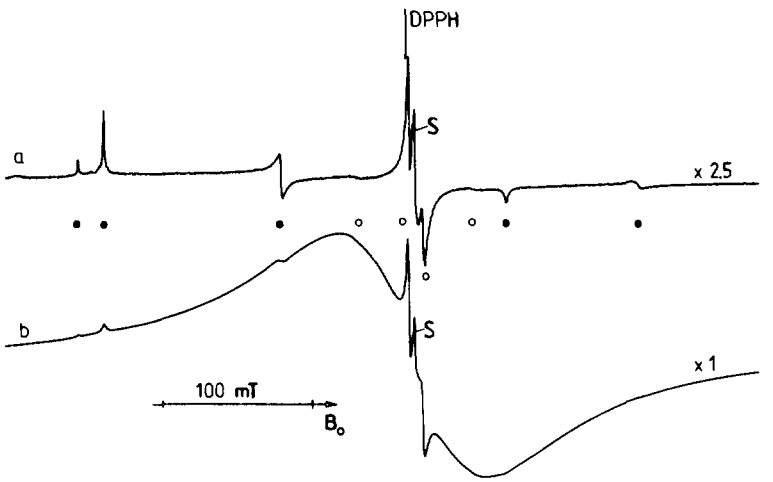

FIG. 11. EPR spectra of calcined samples after TPR (T = 973 K) for total chromium contents of (a) 0.5 wt% and (b) 10 wt%. Cr(III) incorporated into the lattices of rutile (●) and anatase (○) overlaid by a surface resonance of Cr(V) (S). Recording temperature, 293 K.

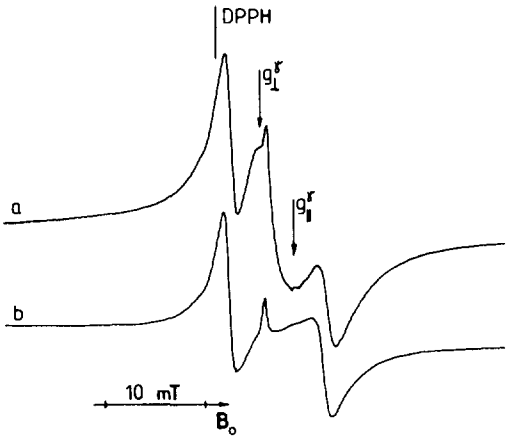

FIG. 12. Cut-off of the EPR spectrum (T = 293 K) for the 1-wt% sample after TPR: (a) before and (b) after treatment with aqueous Na_2EDTA solution. A spectrum similar to (b) is obtained for a recording temperature of 130 K (without previous treatment with solution).

surface complexes, most probably by NO_3^- (reduction to NO_x). The main portion of chromium, however, is deposited on the surface of TiO_2 as a condensation product of $[Cr(H_2O)_6]^{3+}$, i.e., as isolated, dinuclear and/or polynuclear Cr(III) species. With increasing chromium content, the amount of isolated (and/or dimeric) species decreases, whereas the amount and size of agglomerates of "Cr_2O_3" increase.

Although Cr(III) complexes are characterized by their inertness toward ligand exchange reactions, several studies on the hydrolysis of the Cr(III) aquo ion reported that dinulcear and polynuclear hydroxy species are formed with increasing pH (*29, 30*). It has also been reported that even in acidic medium polynuclear (trimeric) Cr(III) species were observed (*30*). This indicates the probability of their formation also in aqueous suspensions of TiO_2 (pH $\approx$ 3.5) especially taking into account the increased temperature and remarkable increasing concentrations by continuous solvent evaporation.

The nucleation is continued by treatment with water, and even when the samples are

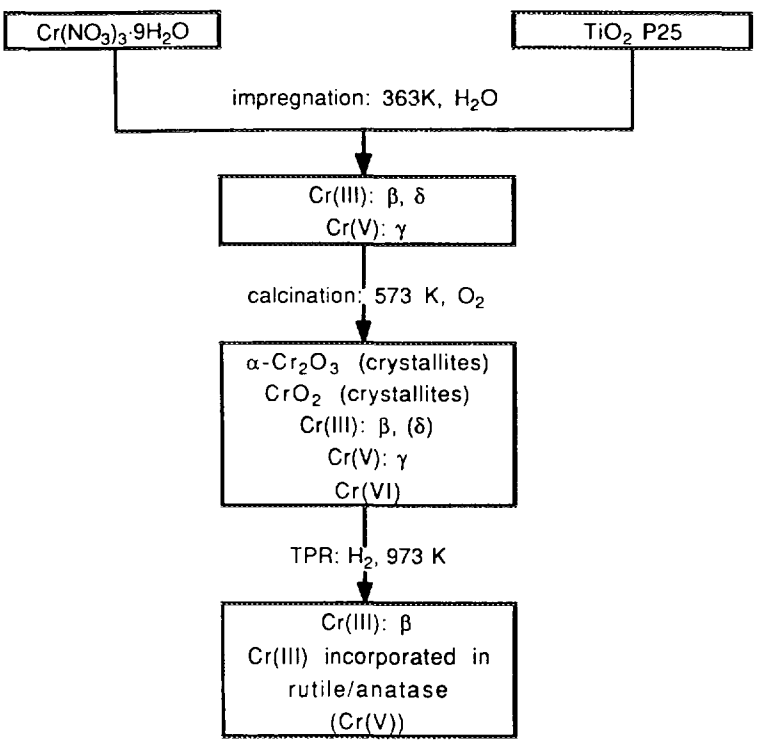

SCHEME 1. Summary of the various chromium species on TiO_2.

stored in air for several months (especially for lower Cr contents). The latter effect illustrates the mobility of the surface species even in "dried" state.

Calcination in an O_2 stream (accompanied by NO_2 formation) gives rise to further oxidation of Cr(III) to Cr(V) and to Cr(VI) (and Cr(IV)) species as well as to continued nucleation of Cr_2O_3 clusters. For very low Cr contents ($\leq$0.5 wt%), nearly all Cr(III) was oxidized; for the higher ones, in general all oxidation states are observable simultaneously.

Quantitatively, for Cr contents $\geq$1 wt%, the most abundant species are clusters of amorphous Cr_2O_3. They differ distinctly in quantity and size with the total chromium content. For 1 to 2 wt%, the EPR spectra indicate a borderline case between very large clusters and small crystallites (antiferromagnetic α-Cr_2O_3), whereas the spectra for 3 to 5 wt% are assigned to large agglomerates of (amorphous) Cr_2O_3. The samples with Cr contents >5 wt% show a collective magnetic behaviour clearly confirming the crystallization of chromium oxide species on the surface of TiO_2. According to our interpretation of the spectra, there exist crystallites of mainly α-Cr_2O_3 on the surface; however, this alone cannot explain all spectral features. The simultaneous existence of ferromagnetic CrO_2 could be a reasonable hypothesis, but needs further confirmation.

The Cr(V) surface complexes detected by EPR have mainly square pyramidal coordination. Cr(V) complexes known from coordination chemistry to be very unstable against disproportionation are clearly stabilized by the surface of TiO_2, as also found for Al_2O_3 and ZrO_2. The very striking temperature dependence of the signal intensity, which to our knowledge has not previously been reported for such surface complexes, shows that the Cr(V) complexes are not isolated but antiferromagnetically exchange coupled to other surface species. It is not possible, therefore, to transfer the relative and absolute intensity of the γ-signal to the actual amount of Cr(V) species. The easy change of the $g_\parallel$ value of only slightly changed conditions confirms the lability of the chromium(V) surface complexes towards ligand exchange. The rapidity with which the γ-signal can be produced and destroyed by oxidation and reduction and the temperature dependence of its EPR spectrum suggests that these species are situated on the surface of the β-phase chromium or at least immediately at the boundary Cr_2O_3/TiO_2. The same is true for the Cr(VI) species forming the outermost layer of the surface, additionally indicated by a colour change from green to yellow upon calcination for low Cr contents and by the easy solubility in water, as well as by complex formation with ethylene glycol.

The Cr(VI) species are shown to be completely reducible by H_2 (TPR, reductive heat treatment), but Cr(V) species only partially so. EPR results as well as H_2 consumption measurements show the reduction to yield mainly Cr(III). Cr(III) ions are incorporated into the rutile (and anatase) lattice at temperatures of about 773 K and higher.

It remains unclear why the agglomerates of Cr_2O_3 found for low chromium contents (1–2 wt%) are larger than those for intermediate ones (3–5 wt%). The difference between the linewidths of the β-signal for our carrier and conditions in comparison to other catalysts (e.g., Al_2O_3, ZrO_2) could be explained by the stabilization of larger agglomerates of amorphous Cr_2O_3, e.g., on Al_2O_3, and/or a more pronounced tendency of crystallization of Cr_2O_3/CrO_2 on the surface of TiO_2 under the given conditions.

ACKNOWLEDGMENT

Financial support of this work by the Swiss National Science Foundation (NFP 24) is kindly acknowledged.

REFERENCES

1. Engweiler, J., Nickl, J., Baiker, A., Köhler, K., Schläpfer, C. W., and von Zelewsky, A., submitted for publication.
2. Evans, J. C., Relf, C. P., Rowlands, C. C., Egerton, T. A., and Pearman, A. J., *J. Mater. Sci. Lett.* **3**, 695 (1984).
3. Evans, J. C., Relf, C. P., Rowlands, C. C., Egerton, T. A., and Pearman, A. J., *J. Mater. Sci. Lett.* **4**, 809 (1985).

4. Amorelli, A., Evans, J. C., Rowlands, C. C., and Egerton, T. A., *J. Chem. Soc. Faraday Trans. 1* **83,** 3541 (1987).
5. Cordischi, D., Indovina, V., and Occhiuzzi, M., *Appl. Surf. Sci.* **55,** 233 (1992).
6. Amorelli, A., Evans, J. C., and Rowlands, C. C., *J. Chem. Soc. Faraday Trans. 1* **85,** 4031 (1989).
7. Poole, C. P., and MacIver, D. S., *Adv. Catal.* **17,** 223 (1967).
8. van Reijen, L. L., and Cossee, P., *Discuss. Faraday Soc.* **41,** 277 (1966).
9. Bertoldi, M., Fubini, B., Giamello, E., Busca, G., Trifirò, F., and Vaccaria, A., *J. Chem. Soc. Faraday Trans. 1* **84,** 1405 (1988).
10. Forni, L., and Oliva, C., *J. Chem. Soc. Faraday Trans. 1* **84,** 2477 (1988).
11. Cimino, A., Cordischi, D., De Rossi, S., Ferraris, G., Gazzoli, D., Indovina, V., Occhiuzzi, M., and Valigi, M., *J. Catal.* **127,** 761 (1991).
12. O'Reilly, D. E., and MacIver, D. S., *J. Phys. Chem.* **66,** 276 (1962).
13. Cornet, D., and Burwell, R. L., *J. Am. Chem. Soc.* **90,** 2489 (1968).
14. Karthein, R., Motschi, H., Schweiger, A., Ibric, S., Sulzberger, B., and Stumm, W., *Inorg. Chem.* **30,** 1606 (1991).
15. Charlet, L., and Karthein, R., *Aquatic Sci.* **52,** 93 (1990).
16. Andriessen, W. T. M., *Inorg. Chem.* **14,** 792 (1975).
17. Van Vleck, J. H., *Phys. Rev.* **74,** 1168 (1948).
18. Anderson, P. W., and Weiss, P. R., *Rev. Mod. Phys.* **25,** 269 (1953).
19. Scaringe, R., and Kokoszka, G., *J. Chem. Phys.* **60,** 40 (1974).
20. Abragam, A., and Bleaney, B., "Electron Paramagnetic Resonance of Transition Ions," Chaps. 3 and 5. Clarendon Press, Oxford, 1970.
21. Pecherskaya, Yu. I., and Kazansky, V. B., *Kinet. Katal.* **8,** 401 (1967); Kazansky, V. B., and Turkevich, J., *J. Catal.* **8,** 231 (1967).
22. Spitz, R., *J. Catal.* **35,** 345 (1974).
23. Ellison, A., and Sing, K. S. W., *Discuss. Faraday Soc.* **41,** 315 (1966); Ellison, A., and Sing, K. S. W., *J. Chem. Soc. Faraday Trans. 1* **73,** 2807 (1977).
24. Cordischi, D., Indovina, V., and Occhiuzzi, M., *J. Chem. Soc. Faraday Trans.* **87,** 3443 (1991).
25. Shapovalova, L. A., Bryukhovetskaya, L. V., and Voevodskii, V. V., *Kinet. Katal.* **8,** 1314 (1967).
26. Köhler, K., unpublished results.
27. Reinen, D., Albrecht, C., and Kaschuba, U., *Z. Anorg. Allg. Chem.* **584,** 71 (1990).
28. Gerritsen, H. J., Harrison, S. E., Lewis, H. R., and Wittke, J. P., *Phys. Rev. Lett.* **2,** 153 (1959).
29. Thomson, M., and Connick, R. E., *Inorg. Chem.* **20,** 2279 (1981).
30. Stünzi, H., and Marty, W., *Inorg. Chem.* **22,** 2145 (1983).